AD NUMBER
AD135345
LIMITATION CHANGES
TO: **Approved for public release; distribution is unlimited.**
FROM: **Distribution authorized to U.S. Gov't. agencies and their contractors; Administrative/Operational Use; OCT 1957. Other requests shall be referred to Arnold Engineering Development Center, Arnold AFB, TN 37389.**
AUTHORITY
AEDC ltr, 16 Jul 1971

AEDC-TN-57-28
ASTIA DOCUMENT NO.:
AD-135345

Copy 1

EFFECTS OF BORON OXIDE DEPOSITS ON AXIAL FLOW COMPRESSOR PERFORMANCE

By

R.O. Dietz, A.H. Hinners, G.F. Dickinson and H.K. Smithson
The Engineering Development Group
ARO, Inc.

October 1957

ARNOLD ENGINEERING
DEVELOPMENT CENTER
AIR RESEARCH AND DEVELOPMENT COMMAND

U S A F

AEDC-TN-57-28
ASTIA DOCUMENT NO.:
AD-135345

EFFECTS OF BORON OXIDE DEPOSITS ON AXIAL FLOW COMPRESSOR PERFORMANCE

By

R. O. Dietz, A. H. Hinners,
G. F. Dickinson and H. K. Smithson

The Engineering Development Group
ARO, Inc.

October 1957

Project 8950 - Task 79450
ARO Project No. 500701

Contract No. AF 40(600)-700 Sup. 6(58-1)

AF - AEDC
Tullahoma, Tennessee

CONTENTS

ILLUSTRATIONS

ABSTRACT

An experimental investigation was conducted at the Arnold Engineering Development Center to determine effects of solid exhaust products from combustion of fuels containing boron upon the performance and operation of axial-flow compressors. A boron-fuel combustor was installed ahead of an axial-flow turbojet engine, and the products of combustion from the combustor were allowed to enter the engine after passing through a water spray cooling system. Deposition of the solid exhaust products in the flow passages of the compressor resulted in reduced compressor pressure ratio, reduced compressor efficiency, and reduced compressor airflow over the range of conditions investigated. Results of this investigation indicate that, in addition to exhaust gas cleaning systems, compressor blade cleaning systems should be installed on axial flow exhausters in altitude test facilities in which boron fuels are burned extensively.

NOMENCLATURE

SYMBOLS

g	Gravitational constant, 32 ft/sec^2
M	Mach number
N	Engine rotational speed, rpm
p	Static pressure, psfa
p_t	Total pressure, psfa
R	Gas constant, ft lb/lb ^oR
r	Thermocouple recovery factor, 0.85
S	Area, ft^2
T	Total temperature, ^oR
t	Static temperature, ^oR
W_a	Airflow, lb/sec
W_f	Fuel flow, lb/sec
W_w	Water flow, lb/sec
δ	Compressor inlet total pressure divided by NACA standard sea level pressure, $p_{t_A}/2116$
η_c	Adiabatic compressor efficiency
γ	Ratio of specific heat at constant pressure to specific heat at constant volume

θ	Compressor inlet total temperature divided by NACA standard sea level temperature, $T_A/518.7^{\circ}R$

STATIONS

0	Ambient duct inlet
1	Burner duct inlet
12	Burner duct outlet
13	Bleed air inlets
A	Compressor inlet
B	Compressor interstage stations
C	Compressor outlet

SUBSCRIPTS

b	Duct burner
c	Engine compressor
i	Indicated

INTRODUCTION

Axial-flow compressors are used in the exhaust systems of at least three altitude engine test facilities in the United States. When engines using boron-containing fuels are tested in these facilities, solid oxide particles flow through the axial-flow exhaust gas compressors. If a high percentage of these boron oxide particles are deposited in the compressor, then compressor performance and operation will be adversely affected. Since the Arnold Engineering Development Center is faced with this problem, an experimental investigation was conducted to determine the extent of boron oxide deposition within an axial-flow compressor and effects of the deposition upon compressor performance and operation.

Water spray scrubbers, which will remove 99.9 percent of the boron oxide particles from engine exhaust gases, are discussed in Ref. 1. Water sprays are used to cool engine exhaust gases between the engine outlet and exhauster inlet in many full-scale altitude engine test facilities currently in use in the United States. Coincidentally the most effective means presently available for removing submicron boron oxide particles from engine exhaust gases utilizes water sprays (Ref. 1). Boron oxide particles formed in ramjet and turbojet combustors vary in size from less than one micron to a maximum of about two microns. Such particles will absorb molecular water from the surrounding gases and convert to H_3BO_3 at the temperatures existing in water spray coolers.

The deposition of submicron carbon smoke particles in axial-flow compressors is discussed in Ref. 2. The tendency of a boric acid crystal to adhere to the smooth metal surface in an axial-flow compressor was considered less than that of carbon smoke. Also, the particle concentrations in the inlet gases used in this investigation are extended to higher values than those in Ref. 2.

The boron oxide concentration allowed to flow through the engine compressor during this test was 8.00×10^{-5} lb/lb of engine inlet air. This is the same as would be encountered in a test facility in which an engine was being tested with all of the air flowing through the engine (i.e., direct-connect testing or ducted nozzle testing) burning with a stoichiometric fuel-air ratio of HEF-3 and an exhaust gas scrubber efficiency of slightly over 99.9 percent.

Manuscript released by authors August 1957.

The results of this investigation show that a high percentage of the boric oxide particles going into the compressor deposited on the compressor. During a 59 minute test with boric oxide particles flowing into the compressor, which was run at a compressor blade tip velocity of about 760 ft/sec (11,000 rpm), the compressor pressure ratio decreased from 2.08 to 1.71, the compressor efficiency decreased from 73 to 61 percent, and the compressor airflow decreased from 19 to 13 lb/sec.

APPARATUS

DESCRIPTION OF TEST EQUIPMENT

The compressor deposition test installation is shown in a photograph, Fig. 1, and as a schematic drawing in Fig. 2.

A J-30 jet engine was used to draw air through a burner duct and engine bleed inlets. Air entered the burner duct at atmospheric pressure and temperature through a bellmouth at station 0. Trimethyl borate azeotrope fuel was sprayed into the burner duct at station 2. The spray nozzle was a commercial full-cone fog type nozzle which was directed either upstream or downstream during different phases of the tests. The flameholder consisted of inconel V-gutters, and a spark plug was used to ignite the mixture. The combustion chamber was 13 1/4 in. in diameter and was 12 ft long.

Cooling water was sprayed on the outside of the combustion chamber in a shower bath arrangement. Dehumidification sprays inside the duct consisted of 25 commercial full-cone fog type nozzles arranged in 5 banks of sprays. The first bank of sprays faced upstream to prevent boron oxide deposition on spray manifolds. Individual banks of sprays could be turned on for a maximum total flow rate of about 500 gpm. Water drained from the system through standpipes located just after the spray section. Two venturi scrubbers in series were located just downstream of the drain section. Each venturi had a fog nozzle located in the throat. These nozzles were not used, however, in these tests. The first venturi had a throat diameter of 7 in; the second, a throat diameter of 7.8 in. Each venturi was followed by a water drain. Entrained water was removed from the air stream by a 14-in. Centrifix line purifier. Burner duct flow then mixed with engine bleed inlet air at station 13. Two valves located at station 13R and 13L could be set to control the amount of air which flowed through the burner duct. The mixture was then drawn through the J-30 turbojet engine and discharged to the atmosphere.

DESCRIPTION OF J-30 TURBOJET ENGINE

The turbojet engine used in this test was a Westinghouse Model 19XB-2B, designated J-30. The engine consisted of an axial-flow ten-stage compressor, a single-cell annular combustion chamber, and a single stage turbine. The engine was operated throughout these tests without a tailpipe. The engine was operated on 80 octane gasoline.

DESCRIPTION OF INSTRUMENTATION

Burner duct instrumentation stations are indicated in Fig. 2. A static pressure measurement at station 1, measured by a Tetra-bromo-ethane (TBE) fluid manometer, was used to determine burner duct air-flow. Fuel was sprayed at station 2, and was measured by a Potter Flow Meter and indicated by a Berkeley E-Put Meter. Combustion chamber temperature was monitored and measured by thermocouples at stations 3, 4, and 5, and indicated on a Brown Pyrometer or Brown Electronik. Three total pressure tubes located at centers of equal area, a wall static orifice, a thermocouple, and a gas sampling probe are located at stations 7, 9, 11, and 12. All pressures at these stations were measured with Kollsman Gauges. Temperatures were indicated on a Brown Electronik.

Gas sampling probes were 1/16 in. ID tubes manifolded and connected by valves to either a vacuum or pressure source. The valves were in the pressure position, when a sample was not being taken, to provide an efflux which kept the tubes clean and free of boron oxide prior to taking a sample. When the valves were switched to vacuum for a timed sample, the vacuum drew the gas through a midget impinger tube, the function of which was to remove entrained water. The sample was then drawn through a 47-mm-diam, type AA millipore filter. The millipore filter is an effective collector of particles down to about 0.01 micron diameter. Flow rates were controlled by a calibrated orifice rated at 2.9 liters per minute located downstream of each filter. This flow control gave approximate isokinetic sampling of the stream.

Material collected by the impinger and millipore was combined and analyzed for boron content, using a d-mannitol, electrometric titration method.

A particle-size sampling station was located at station 6. A pipe with holes drilled streamwise was welded in place across the combustion chamber. Glass slides fastened to a rod could be inserted into this pipe to allow the boron oxide particles to impact on the glass slides. Water sprays upstream of the station were turned off to get a dry sample.

Static pressure orifices upstream of the bleed valves at station 13R and 13L were measured on a TBE fluid manometer to determine bleed inlet flow. The bleed inlet flow could then be added to the burner duct

flow with allowances for moisture and fuel oxide content to determine the flow through the inlet of the J-30.

The J-30 turbojet instrumentation stations are indicated in Fig. 3. Compressor inlet, station A, instrumentation is shown in Fig. 4. Two radial rakes, each containing three total pressure tubes and two thermocouples, were used with wall static orifices located near each rake to determine compressor inlet flow conditions. The total pressure tubes were located at centers of equal area. All compressor inlet pressures were recorded on TBE fluid manometers.

Station B instrumentation consisted of nine compressor interstage static wall orifices to determine the stage static pressure rise. All station B pressures and subsequently described pressures were recorded on mercury manometers.

Station C, the compressor outlet station, had two radial rakes located as indicated in Fig. 5. Each rake was composed of three total pressure tubes and two thermocouples with wall static orifices located near each rake.

Station D had a single total pressure tube located at the turbine inlet.

The tailpipe outlet station, Station E, had two rakes as indicated in Fig. 6. The upper rake consisted of three total pressure tubes, two stream static tubes, and a single thermocouple. A wall static orifice was located near the rake. The lower rake was composed of 5 thermocouples. All temperatures were indicated on a Brown Electronik.

Engine fuel flow was measured by a Potter Flow Meter. A tachometer generator was used to measure engine rpm. Both fuel flow and engine rpm were indicated on Berkeley E-Put counters.

CALCULATION METHODS

Total pressure sensing elements in rakes at the compressor inlet and compressor outlet were located so that an arithmetic average of the pressure sensed by each element produced an area weighted average total pressure. Compressor pressure ratio was taken as the ratio of pressure at station C to pressure at station A.

$$\text{Compressor pressure ratio} = p_{t_C}/p_{t_A} \tag{1}$$

Temperature sensing elements in rakes at the compressor inlet and compressor outlet were located so that an arithmetic average of the temperature sensed by each element produced an area weighted average temperature. Indicated temperature values at the compressor inlet (station A) and the compressor outlet (station B) were used to determine static temperature by use of the equation:

$$t = \frac{T_i}{1 + r\frac{\gamma - 1}{\gamma} M^2} \tag{2}$$

Mach number in Eq. (2) was determined from static pressure and total pressure measurements and Table 1 of Ref. 3. Total temperatures at stations A and B were calculated by use of the equation:

$$T = t\left[1 + \frac{\gamma - 1}{2} M^2\right] \tag{3}$$

Compressor temperature ratio was taken as the ratio of total temperature at station C to total temperature at station A.

$$T_C/T_A = \text{Compressor temperature ratio} \tag{4}$$

Adiabatic compressor efficiency was calculated by use of the equation:

$$\eta_c = \frac{\left(p_{t_c}/p_{t_A}\right)^{\frac{\gamma-1}{\gamma}} - 1}{\left(T_c/T_A\right) - 1} \tag{5}$$

A value of 1.4 for γ was used for all calculations of compressor efficiency.

Compressor airflow was taken as the sum of the burner inlet airflow, bleed inlet airflows, burner fuel flow, and the quantity of water required to saturate the compressor inlet airflow at the temperature and pressure existing at station A.

$$W_{a_A} = W_{a_1} + W_{a_{13L}} + W_{a_{13R}} + W_{f_b} + W_{w_A} \tag{6}$$

Airflow at the burner inlet was calculated by use of the equation:

$$W_a = \frac{g\, p_1\, S_1\, M_1}{\sqrt{T_1}} \sqrt{\frac{\gamma}{R}} \sqrt{1 + \frac{\gamma - 1}{2} M_1^2} \tag{7}$$

Station 1 was a minimum area station immediately downstream of the burner inlet bellmouth and the area was 0.307 ft^2. Total pressure at station 1 was assumed to be equal to ambient atmospheric total pressure p_{t_O}, and was taken from the local barometric reading. Static pressure at station 1 was measured by means of a static pressure wall orifice.

Total temperature at station 1 was assumed equal to local atmospheric temperature.

Airflow at the bleed air inlets, station 13L and 13R, was determined in the same manner as that at station 1; flow areas at station 13L and 13R were 0.545 ft^2 at each bleed. Specific humidity in pounds of water vapor per pound of air for saturation at the temperatures and pressures existing at the compressor inlet, station A, was taken from a specific humidity chart for air. Water flow, W_W, was determined by multiplying the specific humidity by the sum of the burner and bleed inlet airflows.

Thermocouple and temperature recorder accuracy for the test installation was considered to be $\pm 3^o$. Compressor inlet, burner inlet, and bleed inlet pressures were measured with an accuracy of ± 0.75 psfa. Compressor outlet pressures and interstage pressures were measured with an accuracy of ± 3.5 psfa. A negligible error was introduced through the assumption of a constant value of the ratio of specific heats for use in all calculations.

On the basis of visual observation, it was felt that a small amount of liquid water entered the engine inlet when the water sprays and burner were operating. This was especially true for data taken after 1.8 pounds of B_2O_3 had entered the compressor. The primary effect of liquid water entering the compressor inlet would be that of lowering the compressor outlet temperature due to evaporation of the water in the compressor flow passage. Quantitative effects of evaporation of liquid water in the compressor could not be detected through an energy balance between the engine compressor and turbine, which was attempted. If liquid water were entering the compressor, the compressor efficiency calculated by Eq. (5) should be higher than the actual adiabatic compressor efficiency. Therefore, decrease in compressor efficiency determined for test runs in which the burner and water spray coolers were operating was conservative.

Oxide concentrations in the compressor inlet air were determined by withdrawing a sample, isokinetically, at the burner duct outlet for two periods of five minutes each during the deposition test phase of this investigation. Oxide from the sample was collected in a millipore filter, and the quantity collected was determined by titration of the collected sample. Total airflow past the sampling station for the sampling period was determined from aerodynamic instrumentation installed in the burner duct. Ratio of the weight of the B_2O_3 sample collected to the airflow past the sampling station represented the oxide concentration.

TEST PROCEDURE

The overall test program was in three phases:

1. Dry calibration run of the engine compressor with the burner duct and spray cooling system installed, but inoperative. Data were taken at several engine speeds between 6,000 and 16,000 rpm.
2. Operation of the engine compressor with the burner and spray cooling system functioning. Data were taken at intervals corresponding to a specific total B_2O_3 flow into the engine.
3. Calibration of the compressor following deposition of B_2O_3 in the compressor with burner duct and spray cooling system installed, but inoperative. Data were taken at several engine speeds between 6,000 and 12,000 rpm, which was the maximum obtainable.

Prior to the first phase of the test, the engine was operated with the water spray cooling system in the burner duct functioning. At 11,000 rpm, the bleed vanes were adjusted so that about 25 percent of the compressor airflow was through the burner and 75 percent was through the air bleeds. After the air bleeds were adjusted, the spray cooling system was shut down and the initial compressor calibration run was made.

Compressor deposition tests were conducted at an engine speed of 11,000 rpm. At this speed, tip velocity was comparable to the blade tip velocities in a full scale exhauster installed at AEDC. Saturation cooling sprays and subcooling sprays were operated, and the duct burner was ignited while engine speed was held constant at 11,000 rpm. Duct burner fuel flow was adjusted to give the desired concentration of B_2O_3 in the compressor inlet air. Data were taken at specified intervals while burner and engine operating conditions were held as nearly constant as possible. One shut down and restart of the system during this phase of the testing was required to refill the burner fuel storage tank and to clean and adjust the burner fuel nozzle.

Fifty-nine minutes of operation with a total B_2O_3 flow into the compressor of 3.88 lb were accomplished. Following deposition testing the compressor with the duct burner and the cooling sprays inoperative was calibrated at engine speeds up to 12,000 rpm. At this speed, the governor setting was at full throttle. Engine outlet temperatures were probably excessive, but a glassy B_2O_3 coating on the engine tailpipe instrumentation prevented their giving a true indication.

DISCUSSION

Compressor performance and changes in compressor performance due to oxide deposition are presented as functions of rotational speed and amount of oxide allowed to flow through the compressor in Figs. 7 through 15. Use of this method of presenting the data in place of attempting to outline a portion of the compressor characteristics curve was compatible with the quantitative accuracy of the results of this investigation. The sacrifice in quantitative accuracy referred to is not absolute in that the results obtained are quantitatively accurate for the J-30 compressor. However, test facility exhaust gas compressors are usually much larger than the compressor used in this investigation. An accurate method of scaling results obtained during this test was not evolved because of the disparity in centrifugal forces acting on the oxide particles in compressors of different size.

It was concluded that the majority of the solid material entering the compressor during the deposition tests of the compressor was actually in the form of boric acid particles. Temperature and pressure conditions in the spray cooling system downstream of the duct burner were in the range which is conducive to conversion of B_2O_3 to H_3BO_3. Ample water vapor was present in the spray cooling system to meet the requirements of the chemical conversion, and the time required for an oxide particle to flow through the spray cooling system was greatly in excess of that required for the combination of the B_2O_3 and water to take place. Size of the H_3BO_3 particles flowing into the compressor was two microns or less, as indicated by microscopic inspection of a glass slide upon which oxide particles were collected during operation of the duct burner. In addition to this physical evidence, it was concluded from results of an investigation of a similar combustor with trimethylborate fuel (Ref. 4) that the combustor would not produce particles in excess of two microns.

Compressor pressure ratio as a function of corrected engine speed is presented in Fig. 7. Pressure ratio prior to B_2O_3 deposition in the compressor was lower than that for the standard J-30 engine compressor installation because the engine tailpipe had been removed. Pressure ratio would have been reduced much further by removal of the engine tailpipe, if engine inlet pressure had not been reduced by pressure losses in the duct system upstream of the engine. Compressor inlet total pressure prior to deposition testing at a corrected engine speed of 11,000 rpm was 140 psf below atmospheric pressure.

Figure 7 shows that compressor pressure ratio was reduced by deposition of oxide in the compressor flow passages. At a corrected engine speed of 11,000 rpm, the pressure ratio was 2.08 prior to oxide deposition and 1.71 after oxide deposition.

Compressor temperature ratio as a function of corrected engine speed is presented in Fig. 8. Oxide deposition on the compressor resulted in a decrease in compressor temperature ratio over the entire range of rotational speeds investigated. The decrease in temperature ratio was, however, not as great as would have been expected from the decrease in compressor pressure ratio. Figure 9 shows the decrease in overall compressor efficiency caused by B_2O_3 deposition in the compressor. At a corrected speed of 11,000 rpm, the compressor efficiency decreased from about 73 percent to about 61 percent.

Boron oxide deposition in the compressor caused a reduction in compressor airflow as shown in Fig. 10. At a corrected speed of 11,000 rpm, the corrected airflow decreased from about 19 lb/sec to about 13 lb/sec.

Interpretation of the airflow and pressure ratio data presented in Figs. 10 and 7 shows that the compressor characteristic was significantly altered by B_2O_3 deposition in the compressor. A reduction of airflow at constant corrected rotational speed for an axial flow compressor in which the characteristic curve had not been modified would result in an increased pressure ratio instead of the decreased pressure ratio shown in Fig. 7. Pressure ratios obtained were not the maximum pressure ratios available from the compressor for operation either before or after deposition of oxide in the compressor. Pressure ratios obtained were those required to match the other components of the J-30 engine in each case. Effects of other engine components upon the point on the compressor characteristic curve at which the compressor operates did not alter the conclusion that the compressor characteristic curve was modified by B_2O_3 deposition because an increase in compressor pressure ratio after oxide deposition would have resulted in a still greater decrease in airflow.

Compressor pressure ratio, compressor temperature ratio, compressor efficiency, and compressor airflow are presented in Figs. 11 through 14 as functions of the weight of oxide which flowed into the compressor. All of the data presented in these figures are for a corrected compressor speed of 11,000 rpm. Compressor performance decreased rapidly as the oxide flowing into the compressor increased to about two pounds. As the oxide introduced into the compressor increased further from 2 to 3.88 lb, the compressor performance decreased only slightly. Inasmuch as the oxide concentration in the compressor inlet remained relatively constant throughout the test, the compressor performance decreased within thirty minutes to a value which was very near the minimum experienced during these tests.

Compressor stage pressure ratio, as a function of the weight of oxide which entered the compressor, is presented in Fig. 15. Stage pressure ratios tended to remain constant or decrease in the inlet and

lower stages of the compressor and to increase in the higher stages. Boron oxide deposition on the lower compressor stages was much heavier than on the higher stages.

Figure 16 shows the compressor prior to oxide deposition testing, and Fig. 17 shows the compressor after oxide deposition testing had been completed. Boron oxide crystal deposits formed on the pressure surfaces and lifting surfaces of the compressor blades (Fig. 17a and 17b). Boron oxide deposits were much less severe on the higher stages of the compressor. Boron oxide deposits in the lower stages of the compressor stators appreciably reduced the flow passages between blades (Fig. 17c). Deposits accumulated on the leading and trailing edges of the stator blades to a thickness of over one-fourth inch. A portion of these deposits was removed while the compressor was running because the deposits rubbed on adjacent blades. Deposits on the casing were rubbed smooth by the rotor blade tips.

Boron oxide penetrated the labyrinth seal on the compressor outlet bearing. Chemical analysis of the oil in the engine lubricating system at the end of the oxide deposition testing revealed the presence of 14 parts per million of boron compared to no detectable boron in a reference sample of the same oil.

Erosion of the first three rows of rotor and stator blades occurred during the oxide deposition testing of the compressor. Steel surfaces of the blades at the leading edge and from one-fourth to one-eighth inch behind the leading edge were rough and slightly pitted after the oxide deposition tests.

During this investigation, it was observed that liquid water was very effective in removing B_2O_3 deposits from the compressor during operation. Authors of this report were convinced that development of a water spray system capable of preventing significant immediate changes in compressor performance during operation with B_2O_3 particles flowing through it could be achieved.

CONCLUSIONS

This experimental investigation of the effects of B_2O_3 particles contained in the inlet air upon axial flow compressor performance resulted in the following conclusions:

1. Particles of B_2O_3, after passing through a spray cooling system, will adhere to compressor blades and flow passages in sufficient quantities to affect seriously compressor performance.
2. A test duration of about thirty minutes, and an equivalent HEF-3 exhaust product removal efficiency of over 99.9 percent, produced the following changes in compressor performance at a compressor blade tip speed corresponding to those in full-scale axial-flow exhaust gas compressors:
   a. Compressor pressure ratio decreased from 2.08 to 1.71
   b. Compressor efficiency decreased from 73 to 61 percent
   c. Compressor airflow decreased from 19 to 13 lb/sec.

REFERENCES

1. Lewis, George D. "Removal and Recovery of Boric Oxide from Combustion Products of Boron Fuels." UAC Research Department R-0943-3, December 1956. (CONFIDENTIAL)
2. Davidson, I. M. "The Axial Compressor Blade Fouling Problem." National Gas Turbine Establishment Report No. R-36, September 1948.
3. Staff of Ames 1 - by 3 - foot Supersonic Wind Tunnel Section. "Notes and Tables for Use in the Analysis of Supersonic Flow." NACA TN-1428, December 1947.
4. Kibler, G. M. "Research and Development in the Area of Special Fuel Evaluation." General Electric AGTDD Project No. 5-(3-3048), Bimonthly Progress Report No. 5, February 1956. (SECRET)

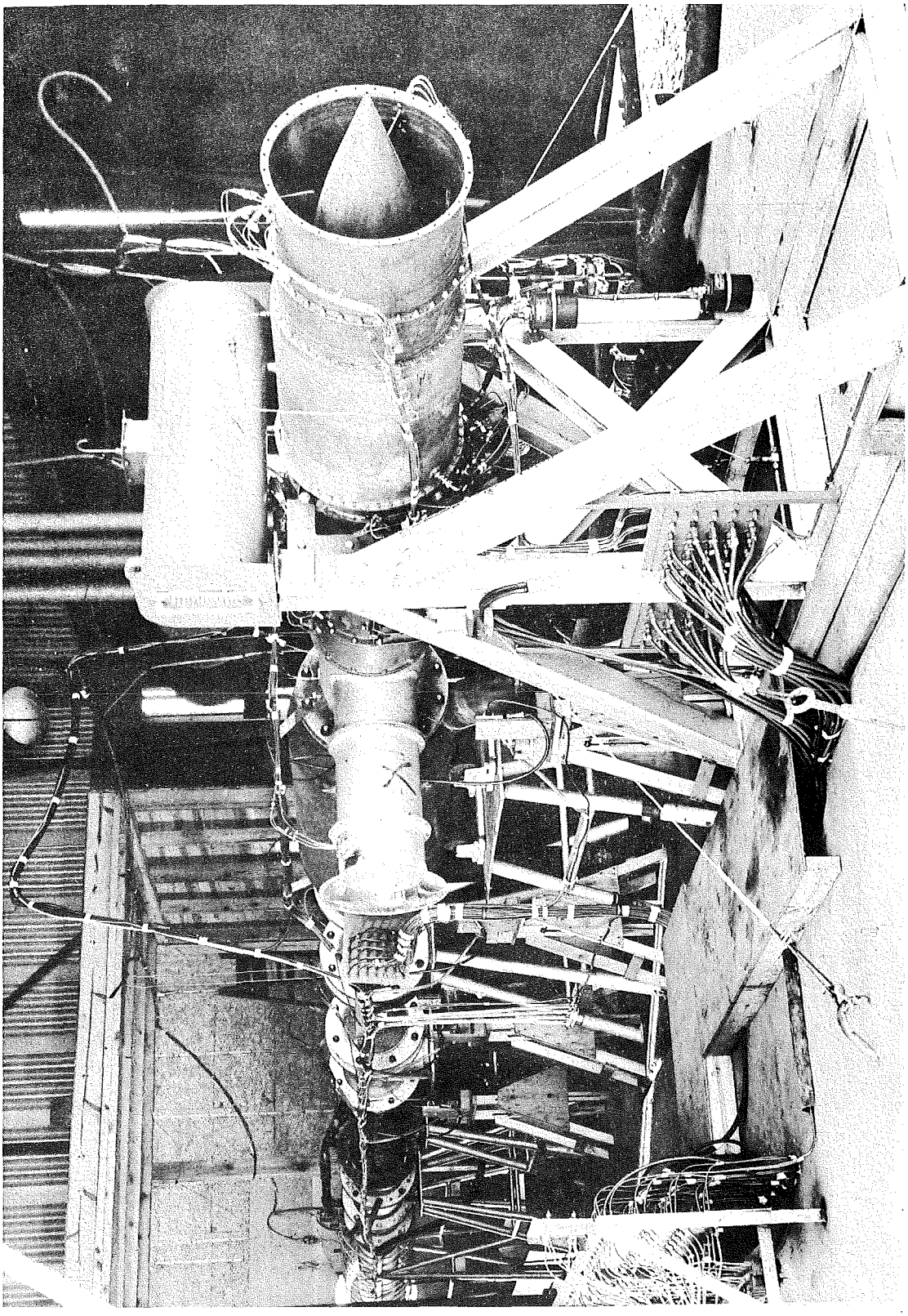

Fig. 1. Compressor Deposition Test Installation

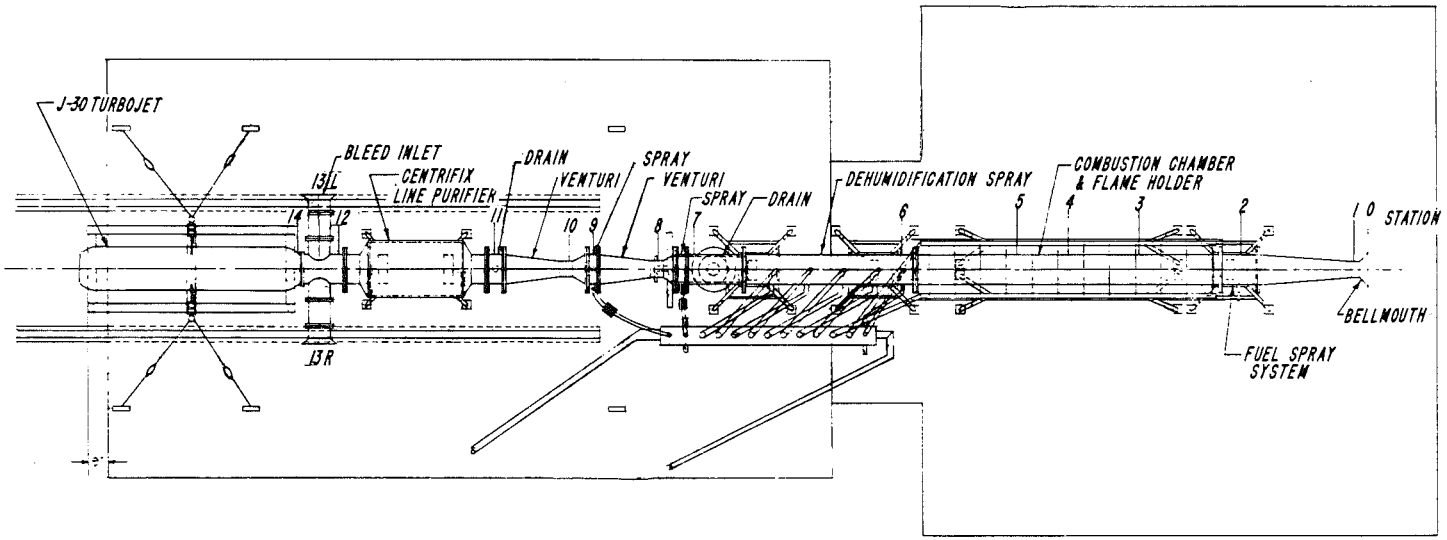

Fig. 2. Assembly of Compressor Deposition Test Installation

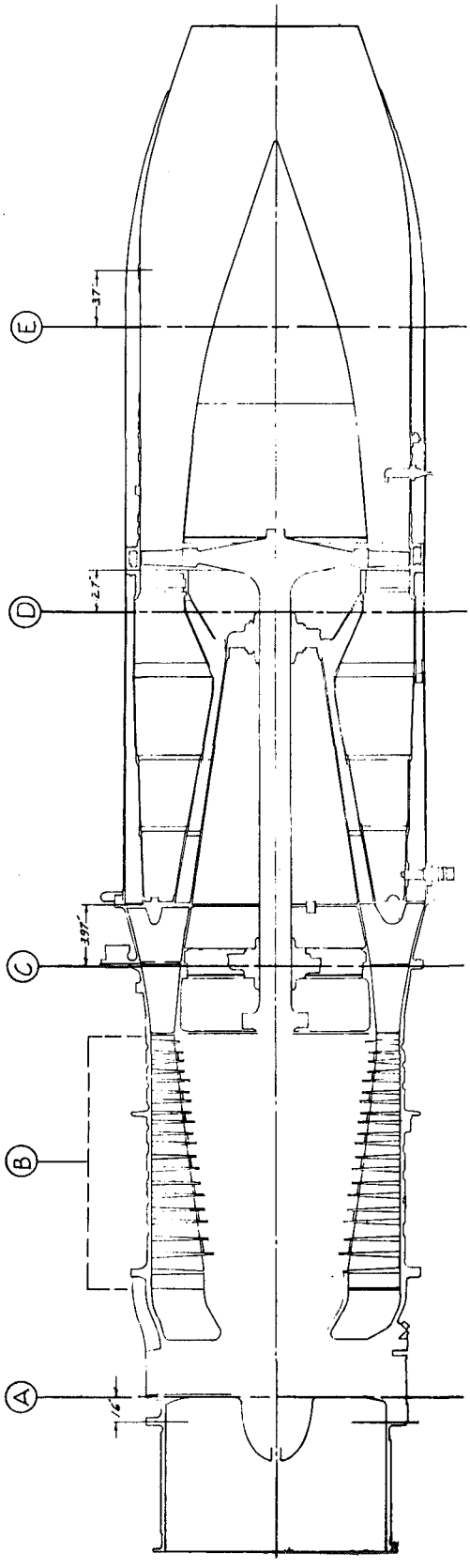

Fig. 3. J-30 Turbojet Instrumentation Stations

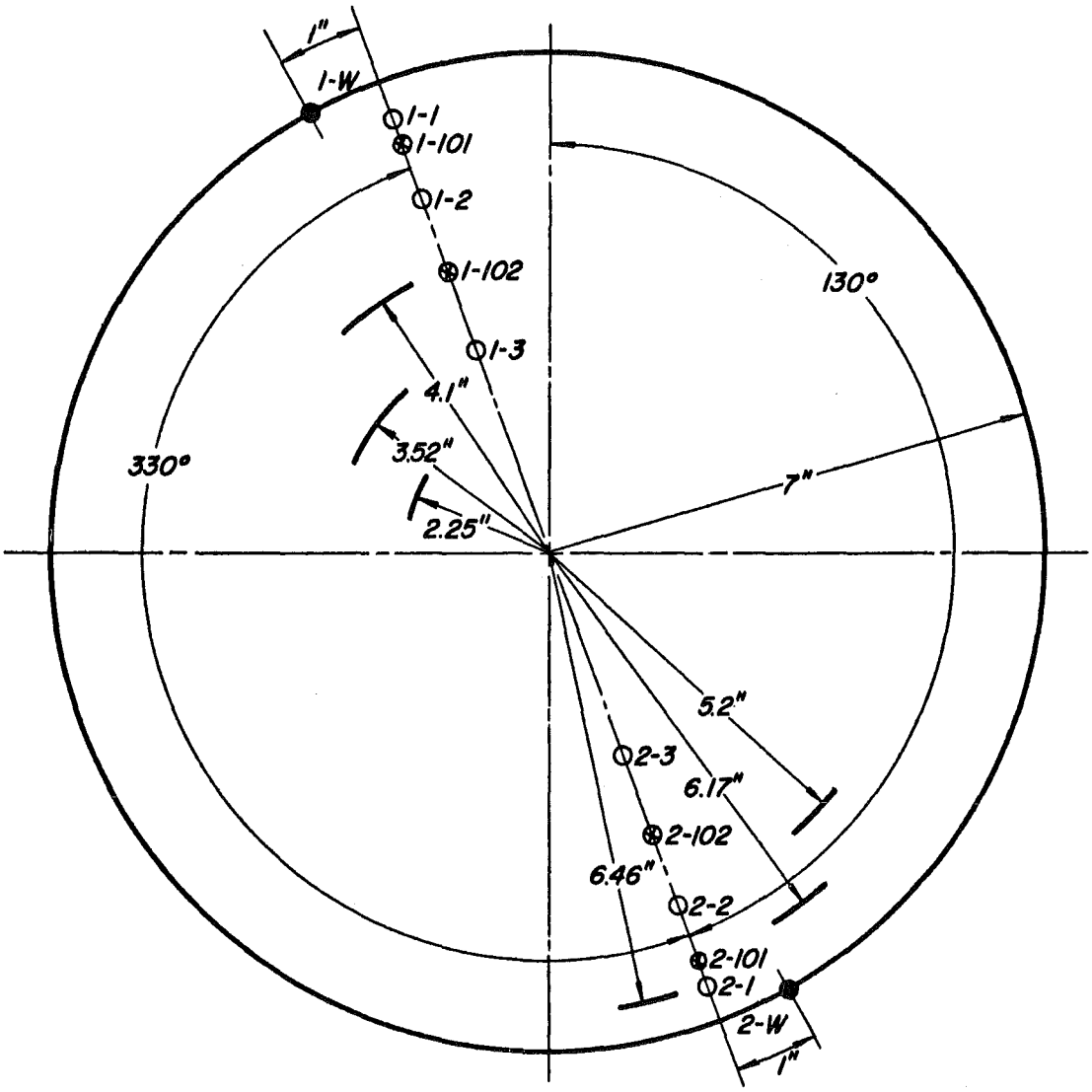

COMPRESSOR INLET STATION - A

SCALE: $\frac{1}{2}$"=1"

1.6" AFT OF THE FRONT FACE OF NO. 1 BEARING SUPPORT HOUSING FRONT FLANGE

○ TOTAL PRESSURE
● STATIC PRESSURE WALL ORIFICE
⊗ THERMOCOUPLE

Fig. 4. Compressor Inlet Station – A

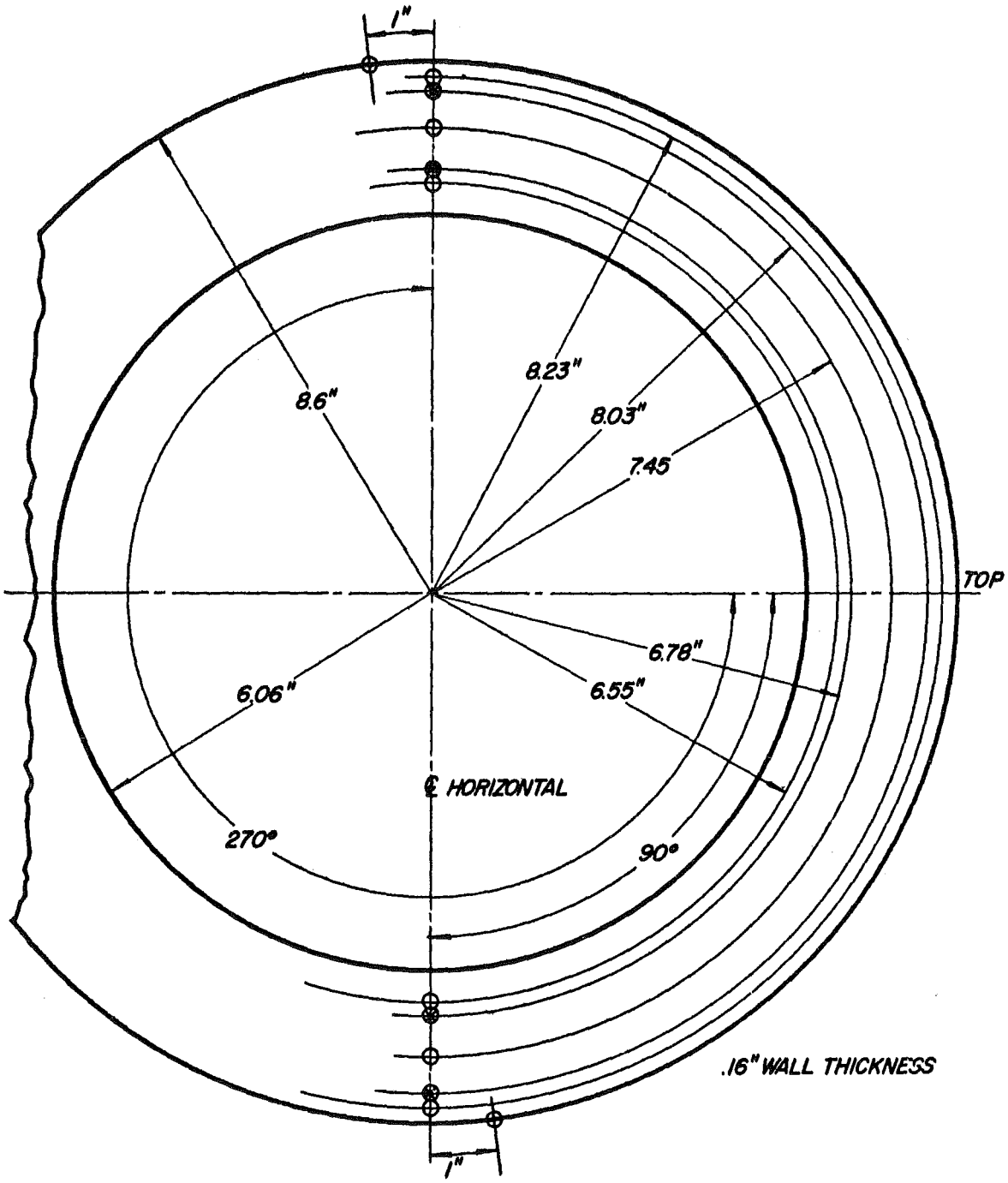

COMPRESSOR OUTLET STATION - C

SCALE: $\frac{1}{2}$"=1"

3 TO 4" RADIAL SPACE BETWEEN ENGINE AND THRUST STAND AT THIS STATION

○ TOTAL PRESSURE
● STATIC PRESSURE WALL ORIFICE
⊗ THERMOCOUPLE

Fig. 5. Compressor Outlet Station – C

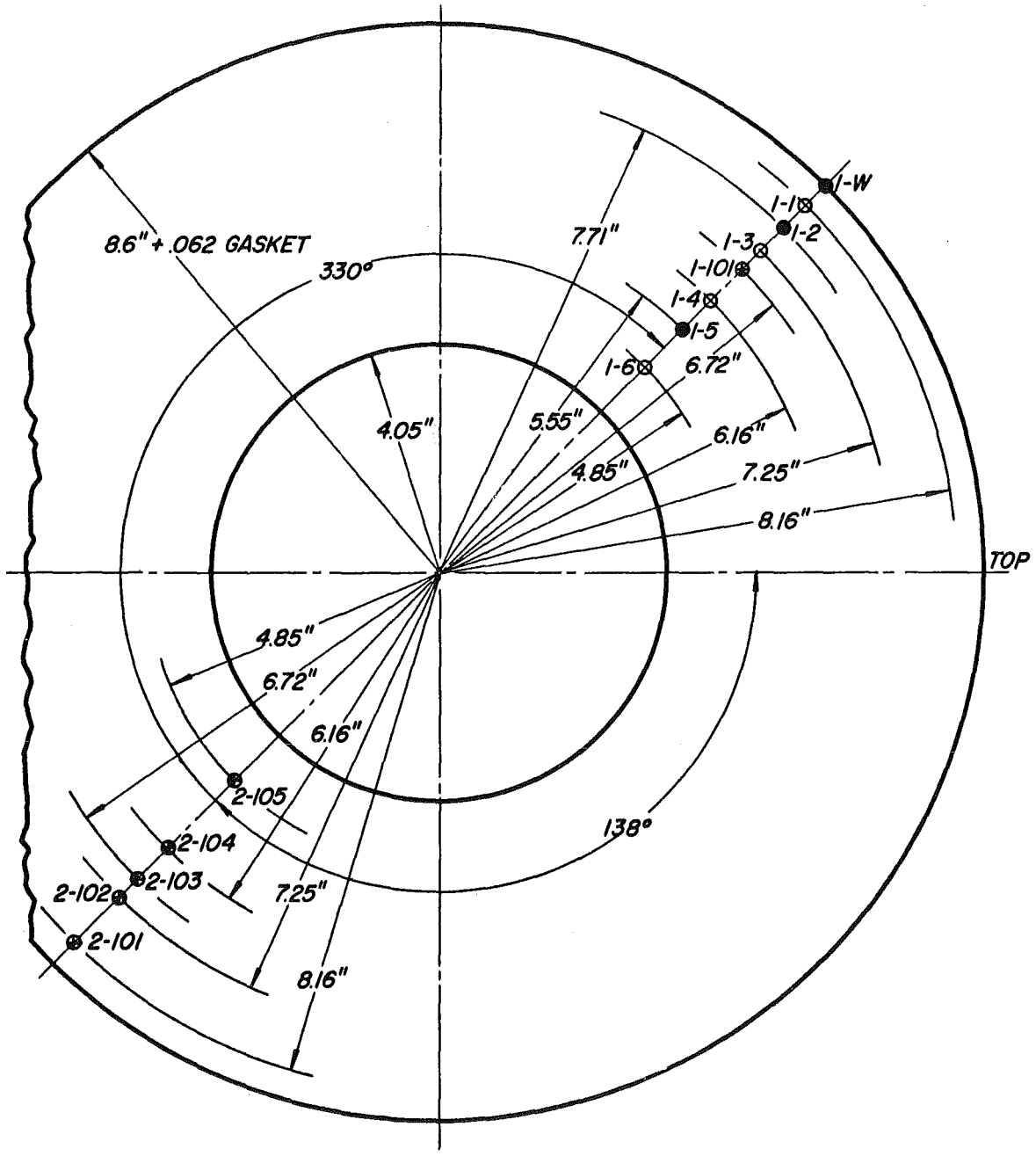

TAIL PIPE OUTLET STATION - E

SCALE: ½" = 1"

3.7" AHEAD OF AFT FLANGE
OF EXHAUST EXTENSION

○ TOTAL PRESSURE
● STATIC PRESSURE
⊗ THERMOCOUPLE

Fig. 6. Tail Pipe Outlet Station – E

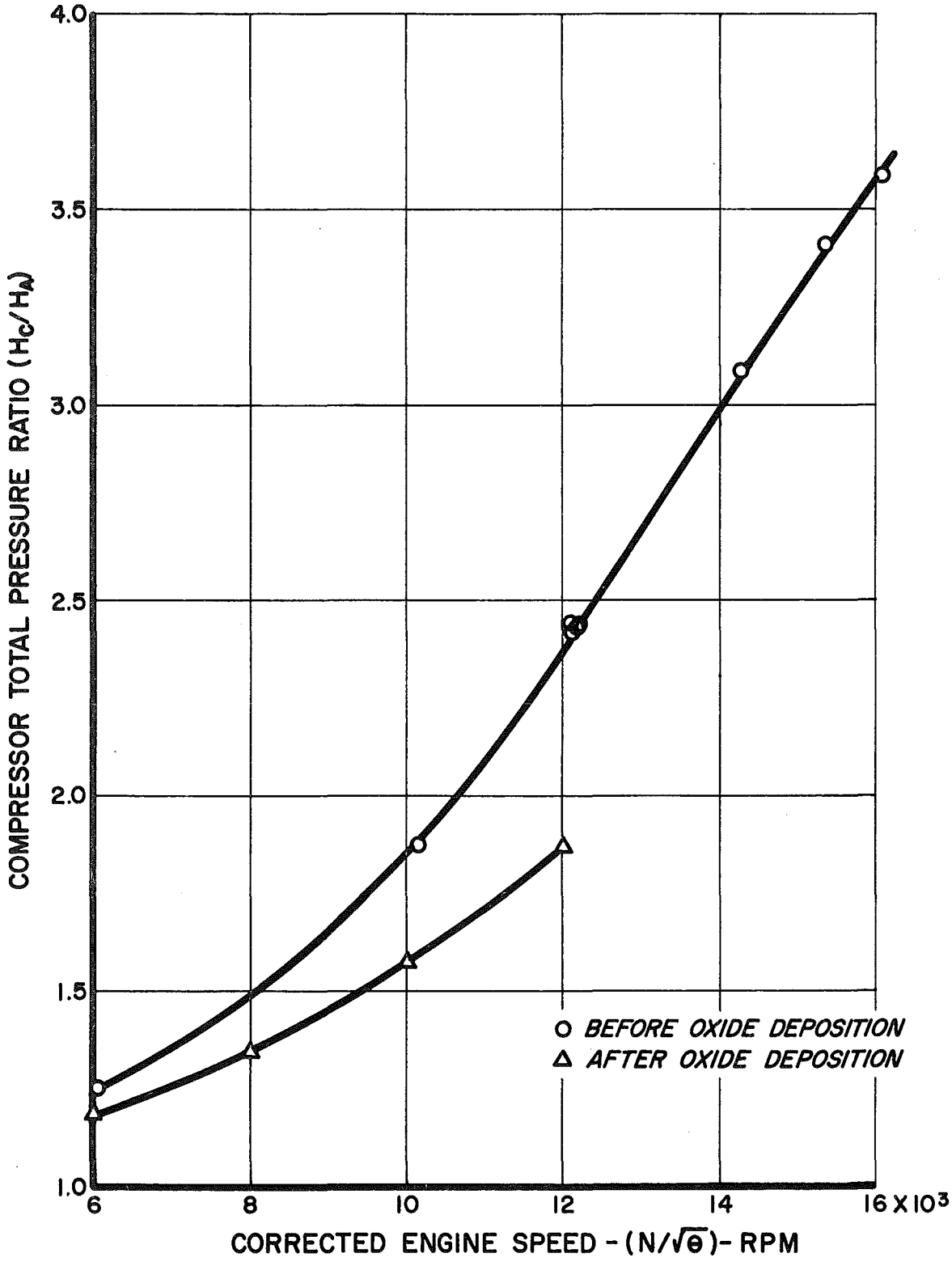

Fig. 7. Effect of B_2O_3 Deposition in Compressor Flow Passages on Axial Flow Compressor Pressure Ratio at Various Rotational Speeds

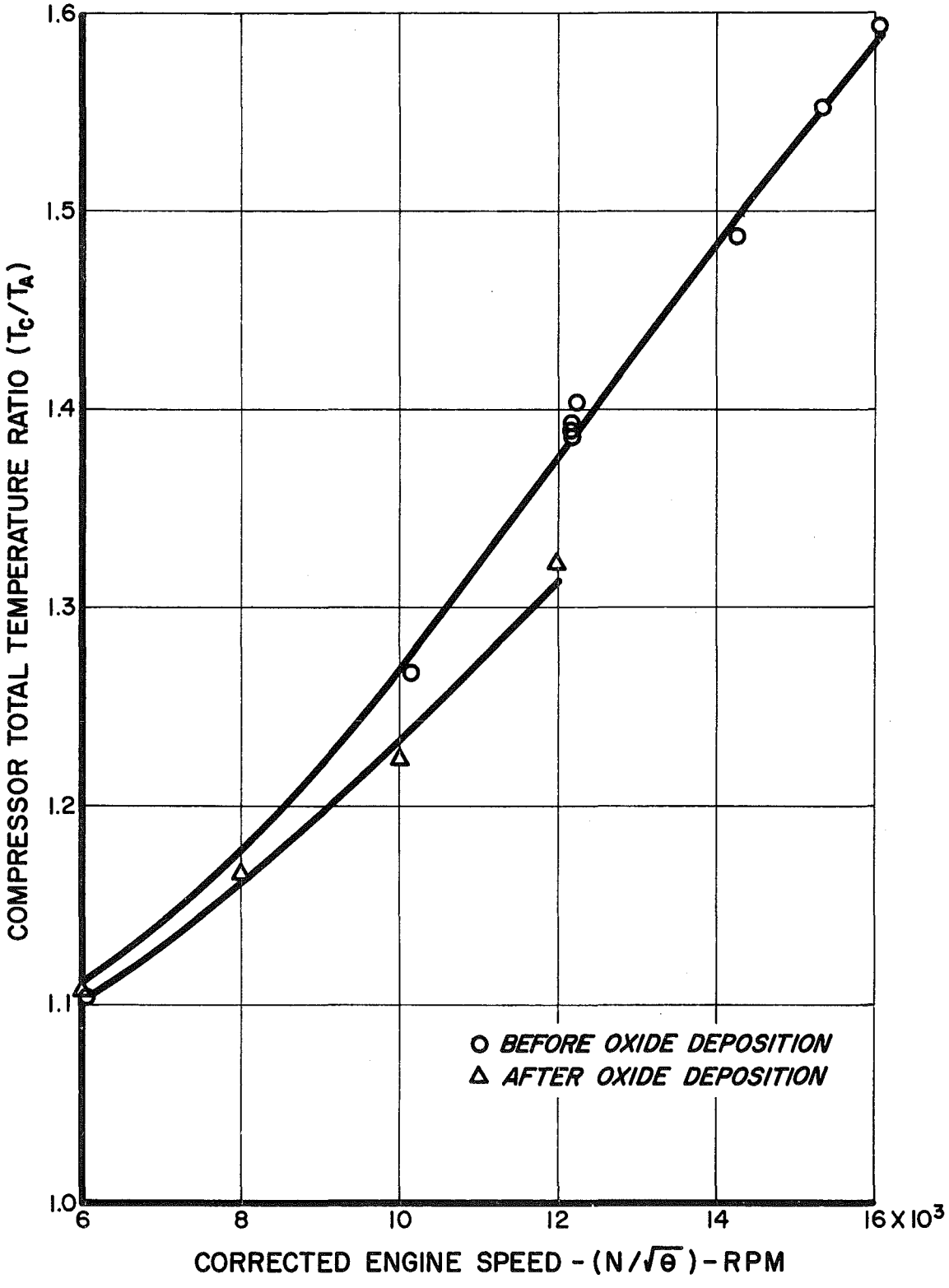

Fig. 8. Effect of B_2O_3 Deposition in Compressor Flow Passages on Axial Flow Compressor Temperature Ratio at Various Rotational Speeds

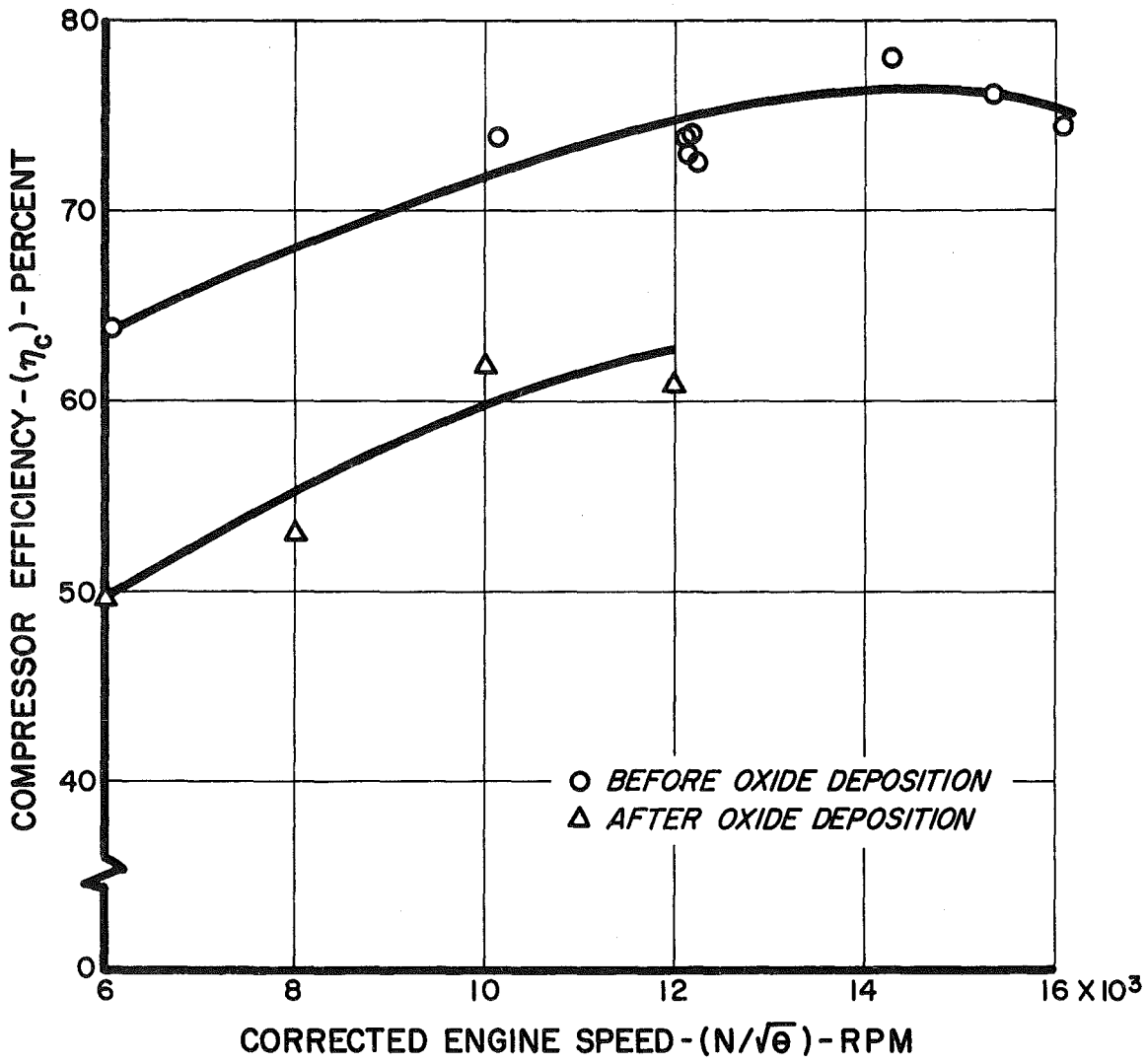

Fig. 9. Effect of B_2O_3 Deposition in Compressor Flow Passages on Axial Flow Compressor Efficiency at Various Rotational Speeds

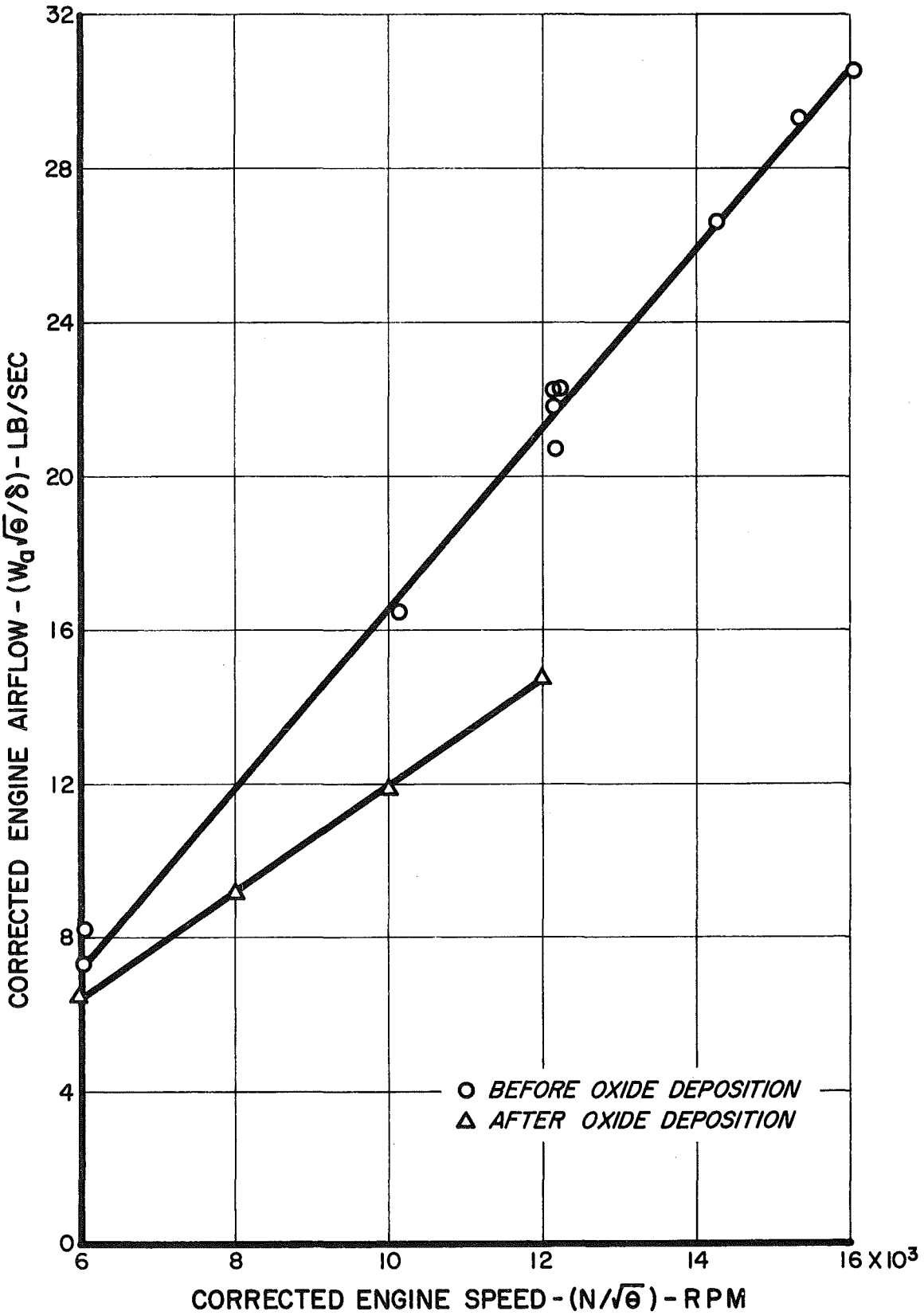

Fig. 10. Effect of B_2O_3 Deposition in Compressor Flow Passages on Axial Flow Compressor Air Flow Rate at Various Rotational Speeds

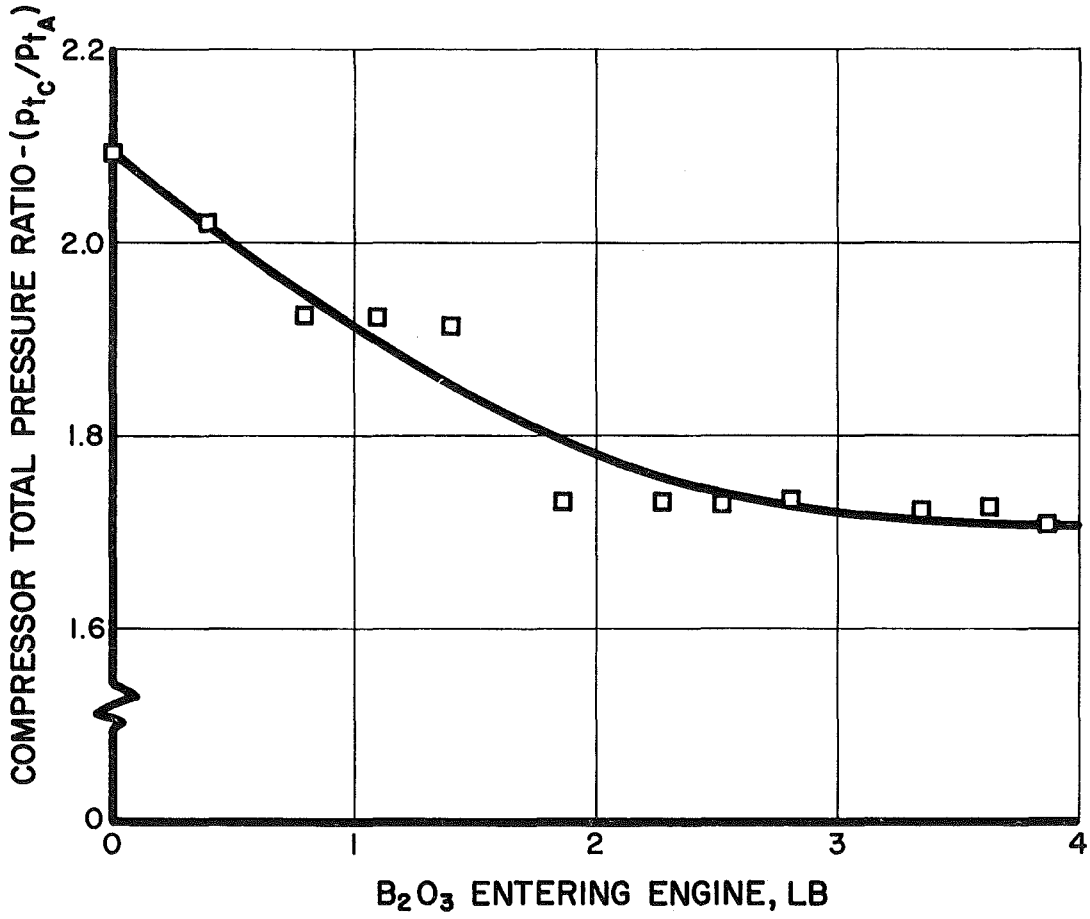

Fig. 11. Decrease of Compressor Pressure Ratio with Increased B_2O_3 Deposition in Compressor Flow Passages

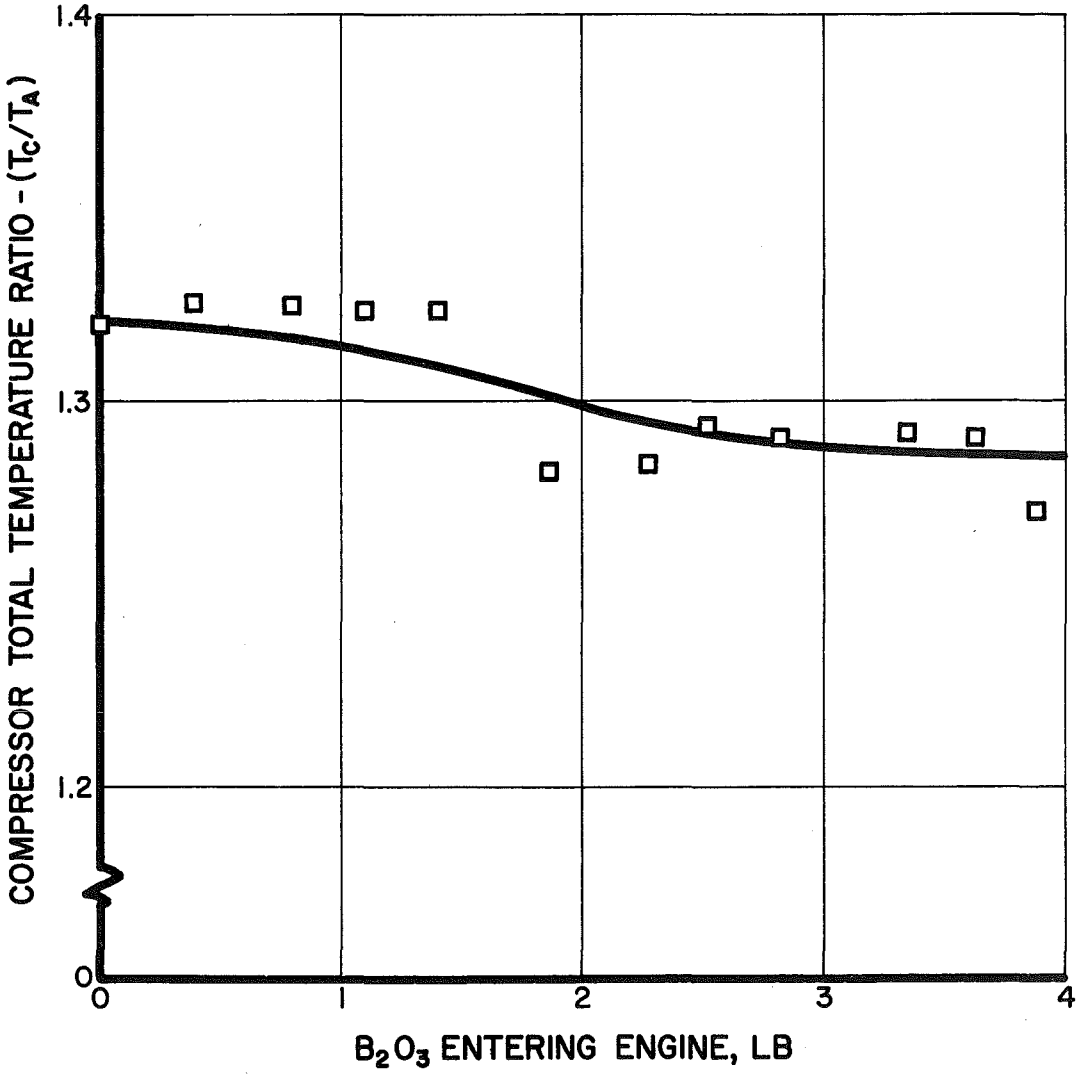

Fig. 12. Decrease of Compressor Temperature Ratio with Increased B_2O_3 Deposition in Compressor Flow Passages

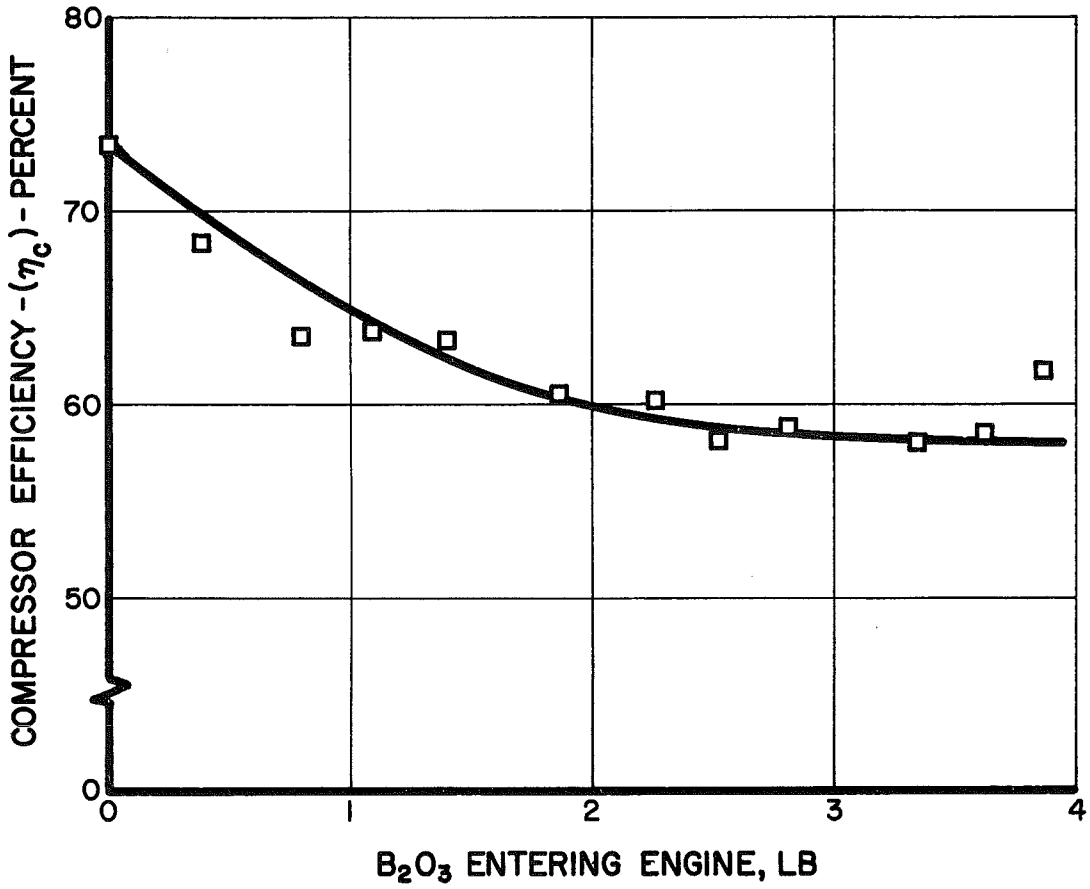

Fig. 13. Decrease of Compressor Efficiency with Increased B_2O_3 Deposition in Compressor Flow Passages

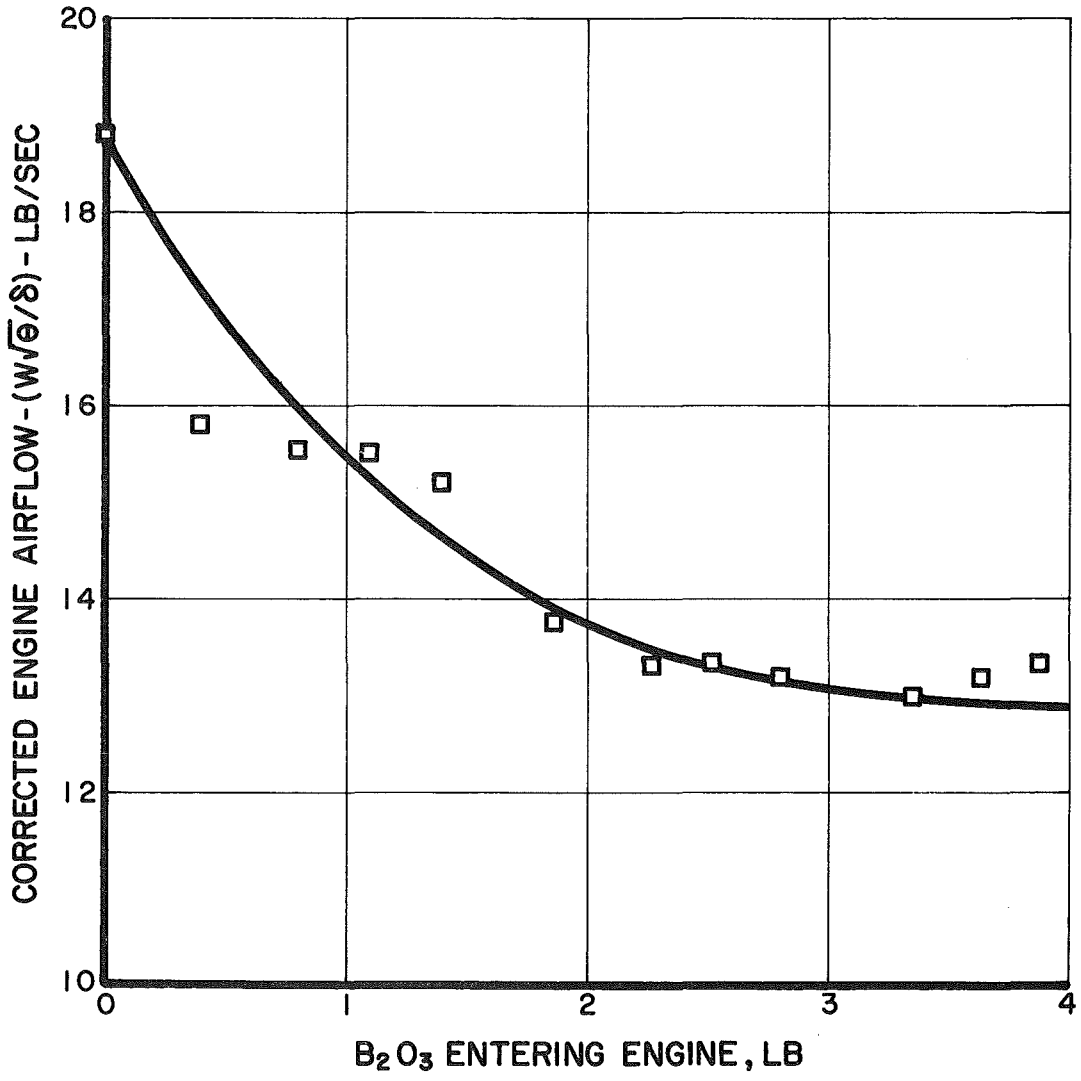

Fig. 14. Decrease of Compressor Air Flow with Increased B_2O_3 Deposition in Compressor Flow Passages

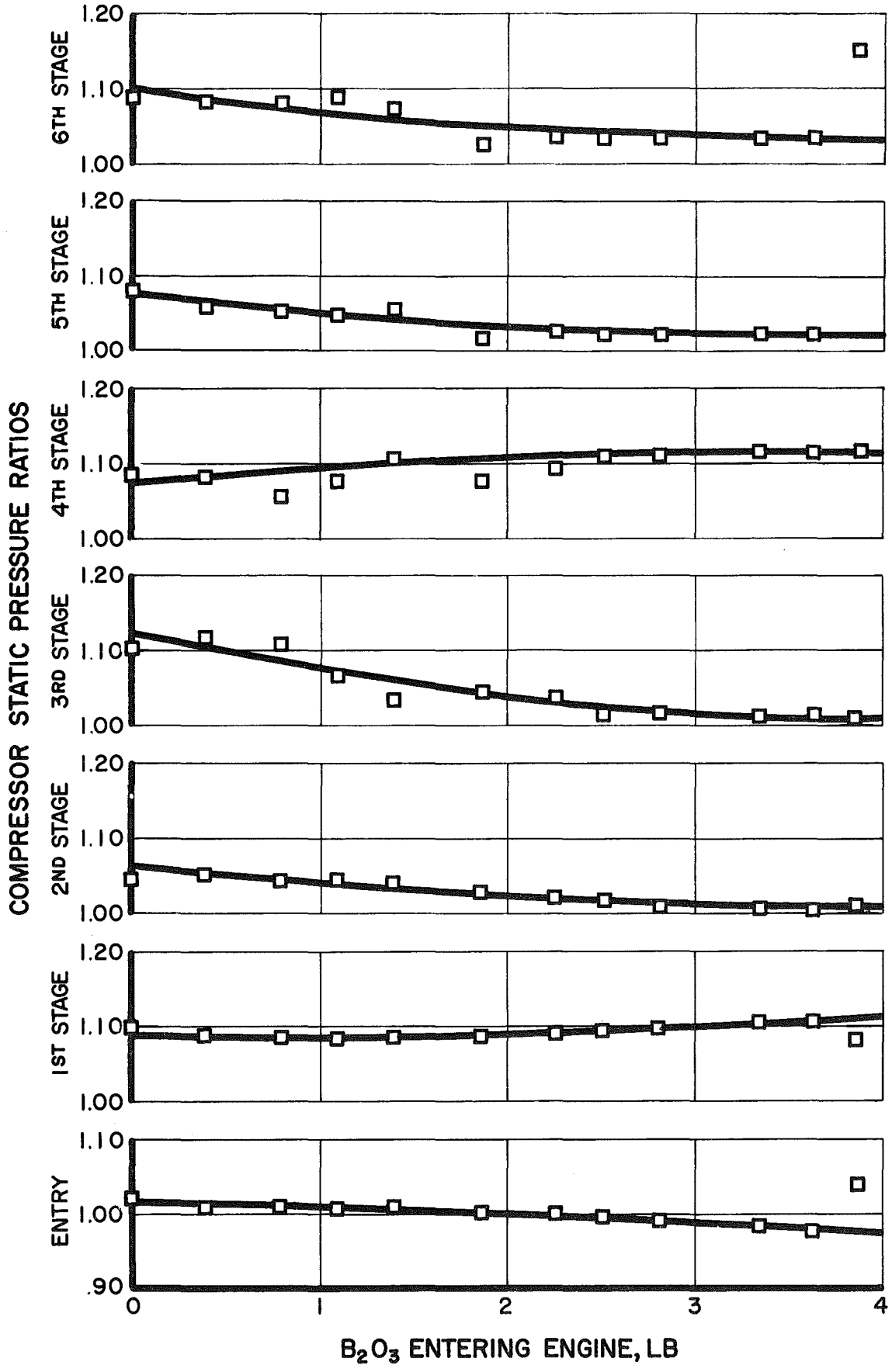

Fig. 15. Change in Compressor Stage Pressure Ratios with Increased B_2O_3 Deposition in Compressor Flow Passages

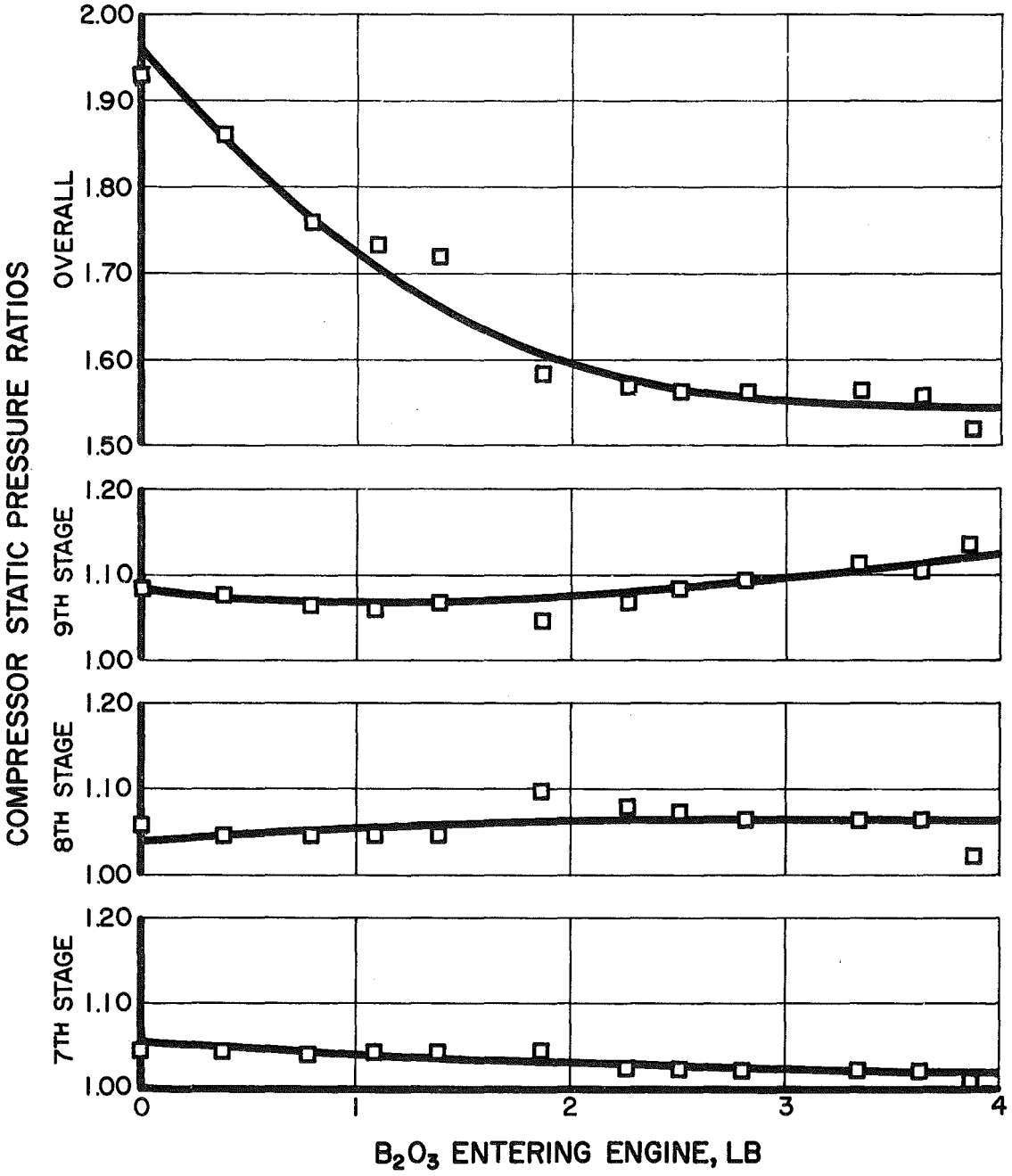

Fig. 15. Concluded

Fig. 16. Compressor Assembly, ¾ Top View before Boron Oxide Tests

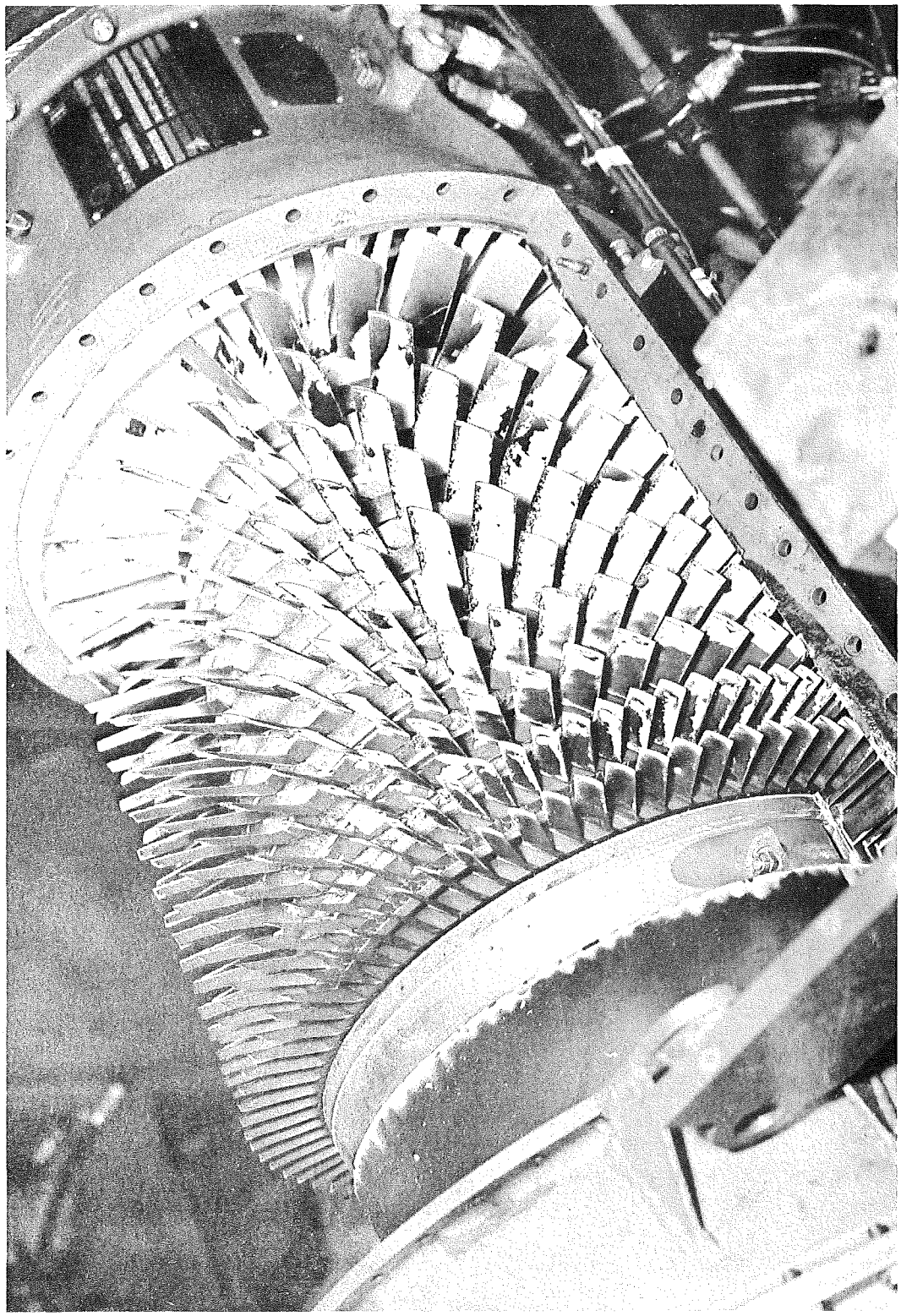

a. Compressor Assembly, ¾ Top View, Contamination after Boron Oxide Tests

Fig. 17. Oxide Deposits in J-30 Engine

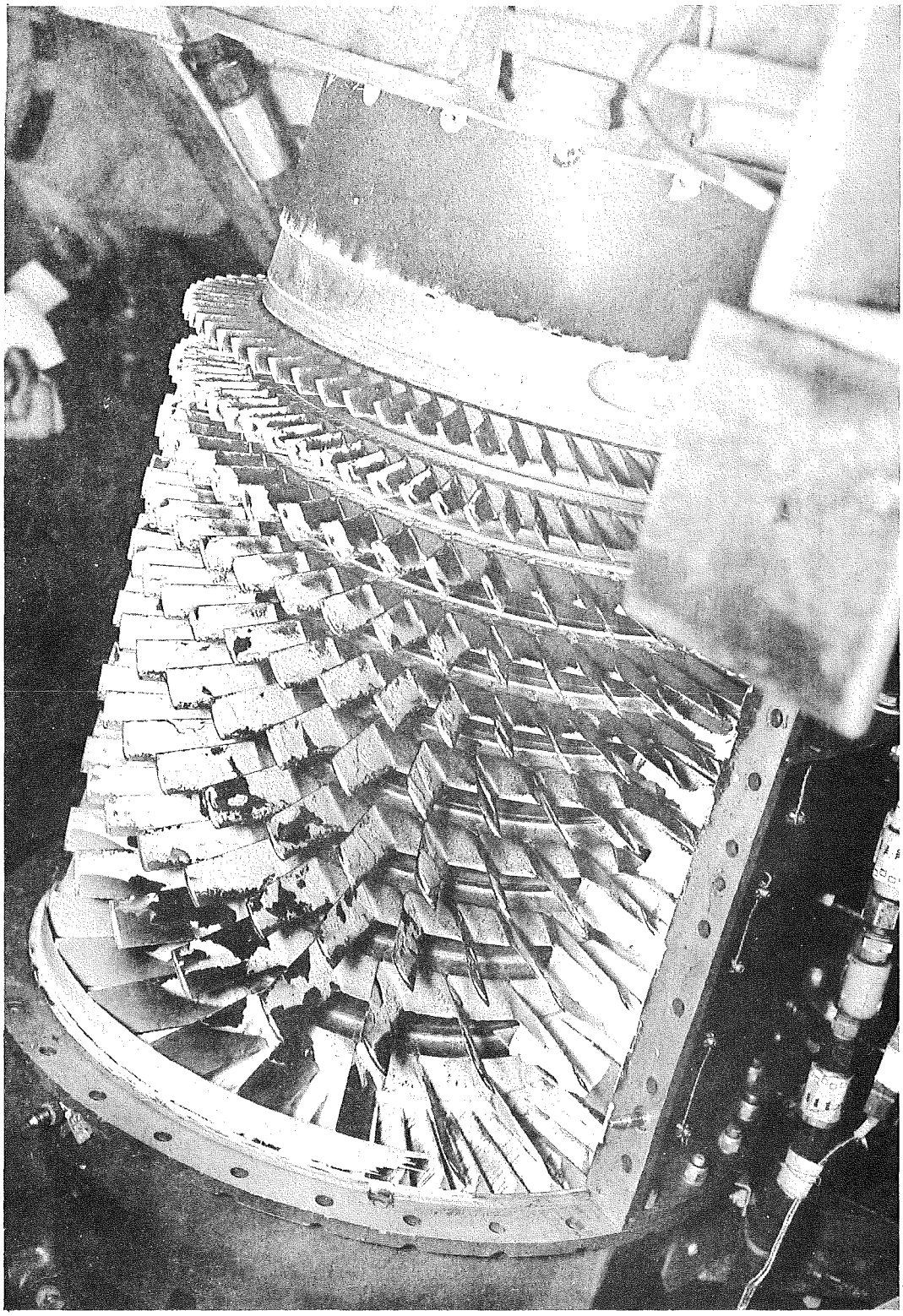

b. Compressor Assembly, Side View, Contamination After Boron Oxide Tests

Fig. 17. Continued

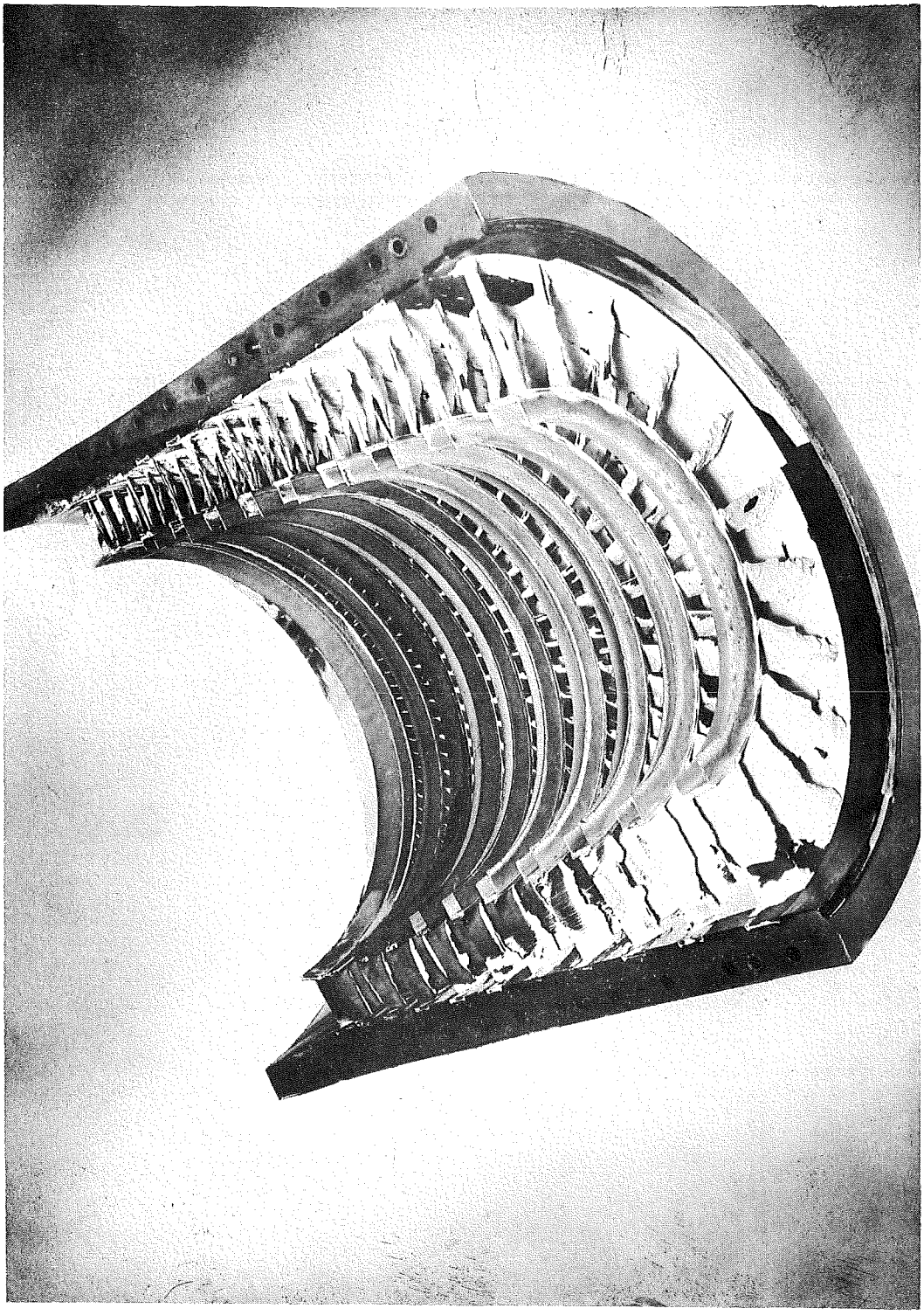

c. Compressor Casing, Contamination after Boron Oxide Tests

Fig. 17. Concluded